10^{-9} mbar. The vacuum chamber is irregular in shape to match the exit beam pipe and the emerging recoils. The rear flange is 5 feet in length. The detectors will mount from large top flanges so as to simplify connections and installation. There is provision for a slow shutter in front of the silicon array to prevent radiation damage during injection. The detector vacuum chamber is currently at an outside vendor for fabrication. Construction of the prototype valve will soon start at IUCF.

FEASIBILITY STUDY OF A STORAGE CELL TARGET

W. Haeberli, W.K. Pitts, J.S. Price, M.A. Ross
University of Wisconsin, Madison, Wisconsin 53706

H.O. Meyer, S.F. Pate, R.E. Pollock,
B. v. Przewoski, T. Rinckel, F. Sperisen, J. Sowinski
Indiana University Cyclotron Facility, Bloomington, Indiana 47408

P.V. Pancella
Western Michigan University, Kalamazoo, Michigan 49008-5151

Experiments with polarized p or d beams on polarized H or D targets become feasible for the Cooler if an internal target of the appropriate thickness is available. To this aim, it has been proposed to use a polarized atomic beam source in conjunction with a storage cell.[1] Such a storage cell, for instance, could be an open tube, mounted along the beam axis, with an intake tube at half length. It has been estimated that by this method a target thickness of $\sim 10^{14}$ atoms/cm^2 can be achieved. This is about 10^3 times more than would be obtained by simply crossing the atomic beam with the stored beam, and would yield a target of a thickness ideal for use in the Cooler.

For a typical output of the atomic beam source of 10^{16} atoms/s, the cell dimensions have to be in the range of 5-10 mm I.D. and 20-40 cm length to provide a feasible target thickness. Since the conductance of the cell scales with D^3, where D is the diameter of the cell, a small diameter is desirable to achieve a large target thickness. However, if the diameter of the cell is too small the cell becomes the limiting element for the machine acceptance. This decreases the luminosity and may cause background from beam particles scattered from the cell walls.

This report describes the results of an experiment (CE26), whose purpose was to test the effects of storage cells on the Cooler performance and to show that experiments with polarized targets are feasible in the Cooler. The experiment was divided into two parts. In the first (phase I) we investigated the effect of a small, variable opening on the machine performance, in the second (phase II) an actual storage cell of realistic dimensions was tested.

For phase I (Feb 1991) we mounted a set of four slits in the A-section of the Cooler (no dispersion, β_x=0.86 m, β_y=1.63 m). The four slits (Left, Right, Up, Down) had remote position readouts and controls. A diffuse gas target was installed in the T-section and was used with several gases (H_2, He, N_2) in order to insert a target of known thickness into the stored beam. The measurement was carried out with unpolarized, 185 MeV protons; kick injection with RF stacking was used. We measured injection performance, ring acceptance, and beam lifetime for various slit openings.

Since the A-section has no dispersion, the energy changes in manipulating the beam during stacking do not cause position changes. Therefore the slits (or a cell) should affect the injection process minimally. The measured accumulation rate with no slits was 9 μA/min, with a 6 mm opening the rate was 7 μA/min and with a 4 mm opening the rate was 5 μA/min. This rate depends sensitively on the ring-setup, on the energy matching between Cooler and cyclotron, on the tune of the injection beamline, and other parameters. Since the accumulation rate was not grossly affected by the slits, it seems to be unnecessary to construct a cell that opens like a clam shell for injection and closes during data acquisition. With the very small slit opening, the accumulation rate depended strongly on the machine setup and was hard to maintain over a long period.

The ring acceptance is measured by exciting a coherent betatron oscillation (by firing a kicker) and observing the associated beam intensity loss. The acceptance is then calculated from the kicker strength that loses half the beam. The acceptance was measured as a function of the positions of all four slits. As seen in Fig. 1, the acceptance with open slits was 11 π·mm·mrad. This is determined by other restrictions in the ring and thus by the ring tune. The A-slits could be closed to 8 mm opening (Left-Right and Up-Down) before the ring acceptance was affected.

The beam lifetime τ is measured by turning off injection after filling and measuring the beam decay on the spectrum analyzer. In Fig. 2, $\sqrt{\tau}$ is plotted versus slit position. When the slit defines the machine acceptance, one expects that $\sqrt{\tau}$ is proportional to the distance between the slit edge and the stored orbit. Again, the A-slits could be closed to 8 mm before affecting the beam lifetime.

The luminosity for an internal gas target can be written as:[2]

$$L = N_{in} \cdot \tau \cdot X_t \cdot f_R$$

where N_{in} is the accumulation rate, f_R is the orbit frequency and X_t is the target thickness in atoms/cm^{-2}. For maximum luminosity the product $\tau \cdot X_t$ must be maximized. In Fig. 3, $\tau \cdot X_t$ is plotted versus X_t for several gases. Using the above accumulation rate, we find, for instance, that for hydrogen gas and 185 MeV protons, a luminosity of 10^{29} is achieved.

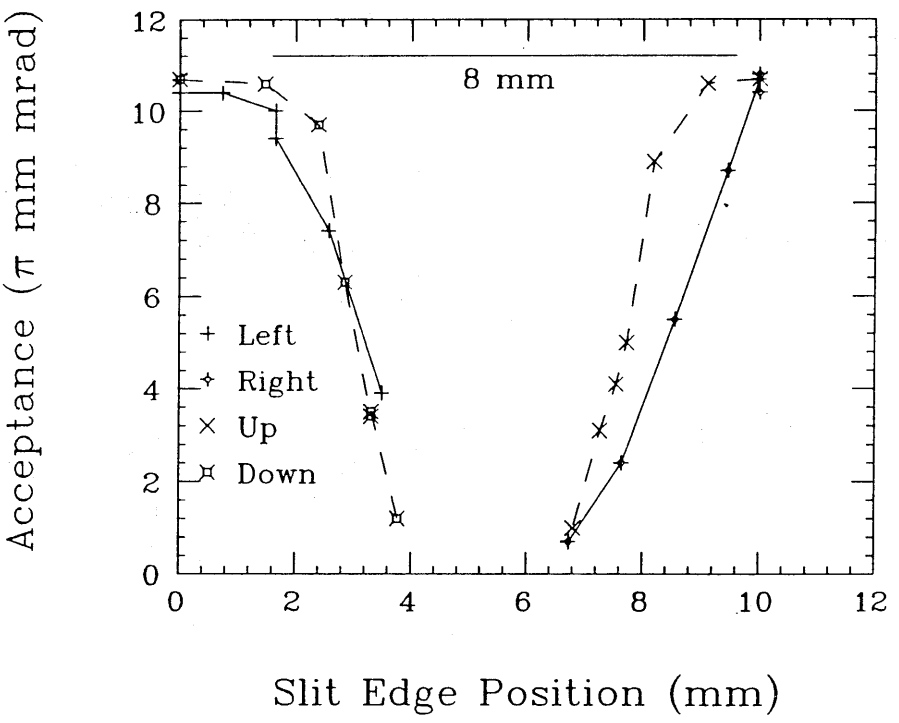

Figure 1. Ring acceptance for four slit jaws vs. slit position. Each jaw was moved individually.

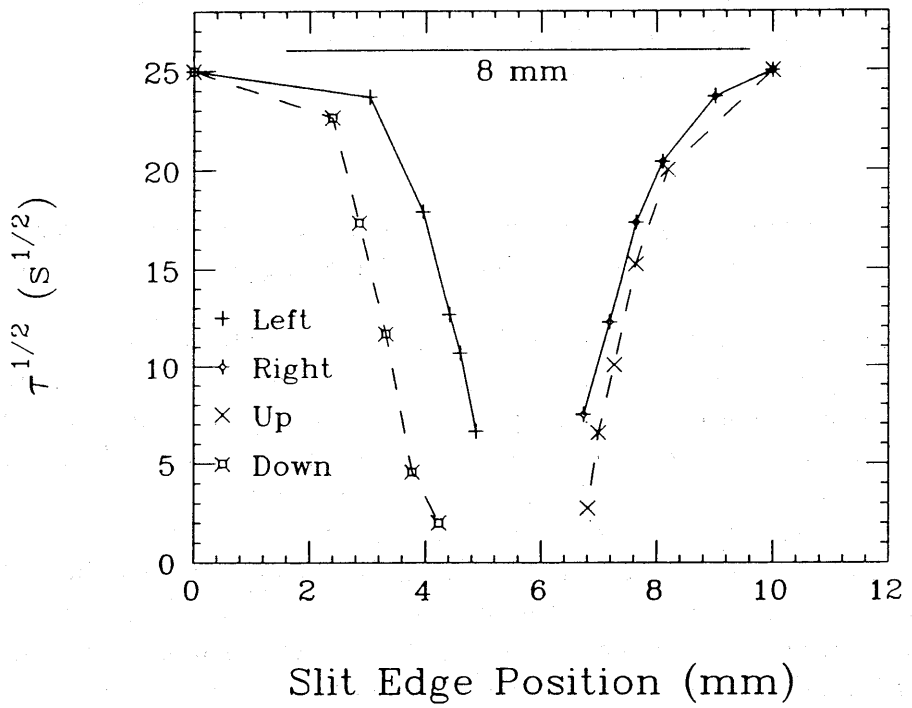

Figure 2. $\sqrt{\tau}$ for four slit jaws vs. slit position. The data were taken simultaneously with the data in Fig. 1.

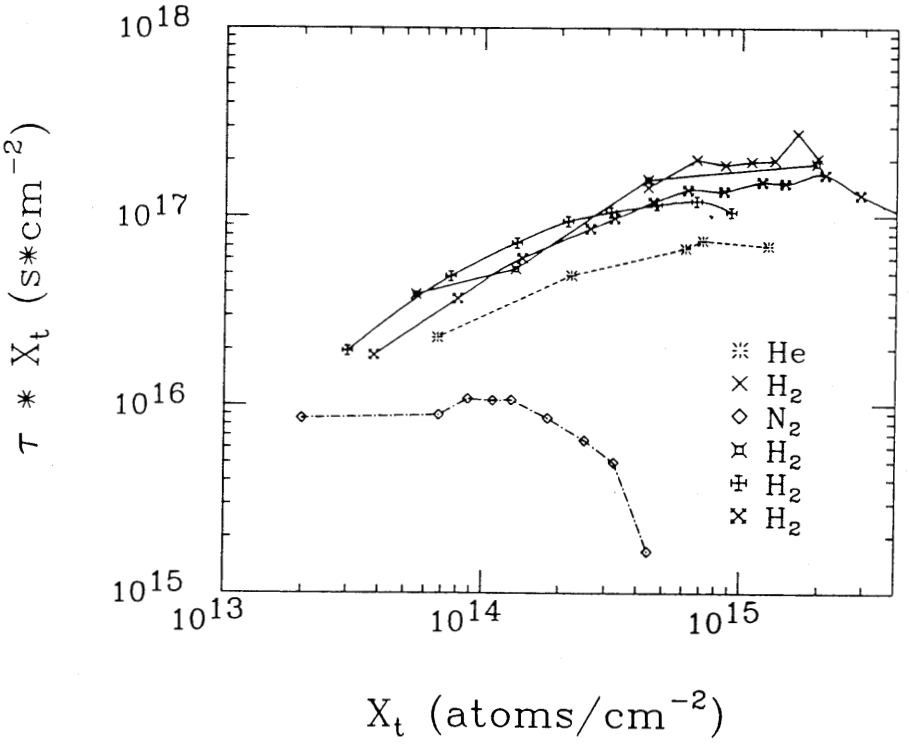

Figure 3. The product of $\tau \cdot X_t$ vs. X_t for 185 MeV protons. At the maximum, the luminosity is optimized. The four curves labelled H_2 show measurements taken at different times, but under the same experimental conditions.

Note, that the curves change slowly over a large target thickness range, implying that a change in target thickness is compensated by a lifetime change and therefore the luminosity stays roughly constant.

In phase II (May 1991) a cell with realistic dimensions was tested in the A-section. The details of the setup are elsewhere in this report. The goal of the run was to prove the feasibility of a measurement of C_{NN} for pp scattering. A sufficient luminosity for this experiment ($5 \cdot 10^{28}$ cm^{-2}s^{-1}) can be achieved with a cell of 8 mm I.D. and 24 cm length. A cell of these dimensions was made from 8.95 mm O.D. aluminum tube. It was aligned with respect to the beam axis using a telescope mounted at the corner downstream from the cell. The cell had a 2 mm I.D. feedtube connected to the midpoint and two openings, 22.5 cm long and 0.5 cm high, on either side which were covered by 1.5 μm thick aluminized mylar windows. Position monitors in the nearest quadrupole magnets as well as just upstream and downstream of the cell were used to determine the beam trajectory through the cell. The cell could be removed from the beam path during machine tuning.

The cell was fed with hydrogen gas at flow rates between 10^{16} and 10^{17} molecules/s; the lower value corresponds to a typical flow of polarized atoms. The test was performed

with an rf-stacked, 185 MeV proton beam. The following detector arrangement was used to detect scattered and recoil protons in coincidence. An array of 8 E-detectors (158 cm downstream from the center of the cell) that covered an angle range of 2°-16° allowed a crude determination of the scattering angle ($\delta\theta = 2°$) of the forward going proton. A ΔE detector was positioned at the exit window (0.13 mm stainless steel) of the chamber. An array of 3 μ-strip detectors (each one 40 mm high, 60 mm long, 7 strips per detector), mounted at a distance of 55 mm from the cell axis, was used to detect the recoiling proton. The μ-strips provided information about the origin of a pp event along the z-axis. The trigger condition was a coincidence between the ΔE-, any one of the E-detectors, and any one of the μ-strips. Figure 4 shows the kinematic locus for pp scattering after applying software cuts. When the cell was filled with He gas a locus from p+^{4}He scattering was observed but no pp locus was visible. This demonstrates that the contribution from pp scattering in the mylar windows of the cell is negligible for the present measurement.

Since the pressure in the cell drops linearly as a function of the distance from the center (location of the feed tube); one expects a triangular gas density profile along the cell. Figure 5 shows the distribution of scattering events along the z-axis. In this sample, protons scattered by $4°-11.3°$ are included (corresponding to four E elements). This measurement was obtained with a flow rate of 1.2×10^{17} molecules per second. The measured distribution is compatible with the expected triangular shape. The density at the top of the triangle was obtained from a measurement of the gas pressure in the center of the cell.

In summary, we have demonstrated that the adequate luminosity can be achieved and that pp scattering events can be cleanly identified. It still needs to be shown that with a detector system that covers a larger solid angle, and with increased beam intensities, the possible problem of beam protons scattering from material close to the beam is manageable.

1. W. Haeberli, Proc. Int. Workshop on Polarized Ion Sources and Polarized Gas Jets (Tsukuba, Japan, February 1990), ed. Y. Mori, KEK Report 90-15, p.35.
2. H.O. Meyer, 19th INS Int. Symp. on Cooler Rings and their Applications (Toyko, Japan, Nov., 1990).

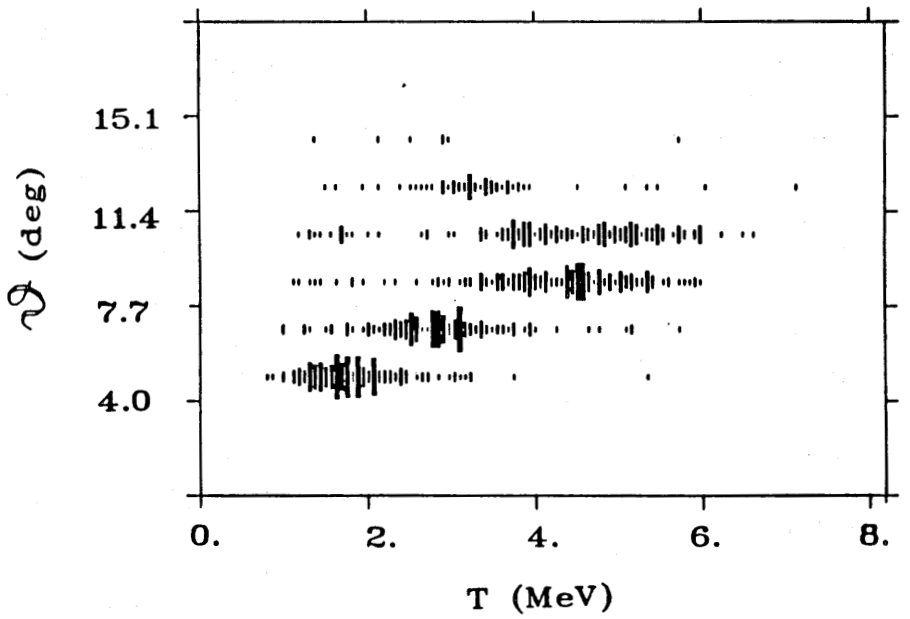

Figure 4. Kinematical locus for p+p scattering for a feedrate of 10^{16} molecules/s into the cell.

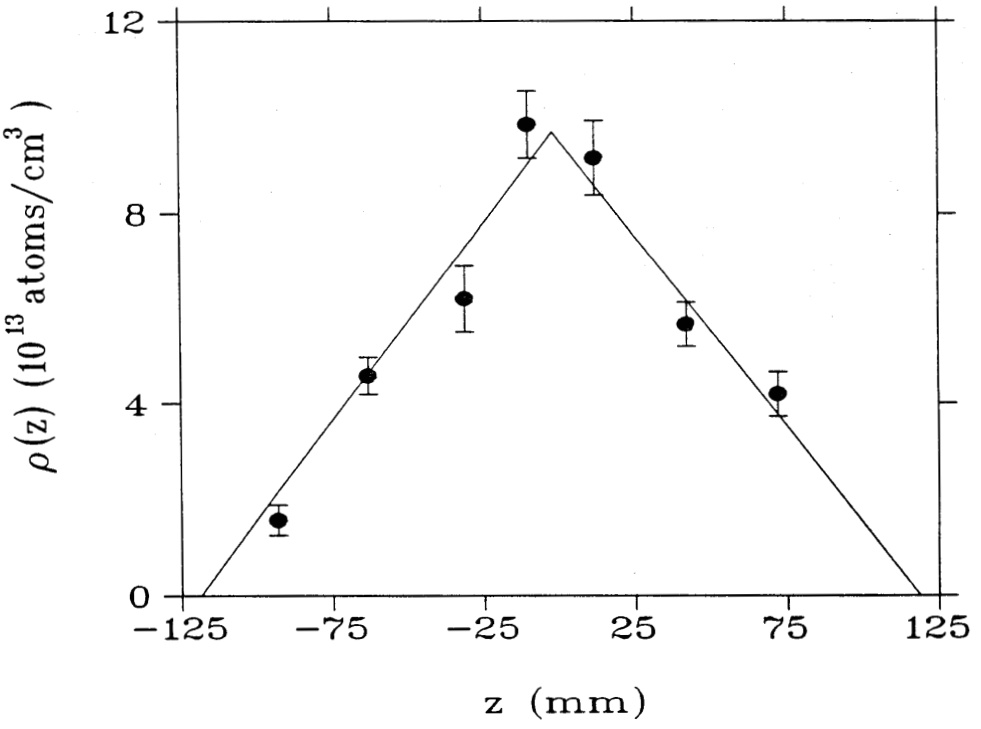

Figure 5. Target gas density along the axis of the cell, inferred from the measured number of pp scattering events. A triangular shape is expected from gas dynamics. The target thickness in this case is 1.2×10^{15} atoms/cm^2